Carola Kruthoff, Jorge Sánchez, Jonathan Krauß, Tobias Gerach, Cristian Barrios Espinosa, and Axel Loewe*

Evaluating the Effects of Left Bundle Branch Block in an Electromechanical Heart Model

https://doi.org/10.1515/cdbme-2025-0199

Abstract: Left bundle branch block (LBBB) refers to a delayed or blocked impulse transmission through the left bundle branch of the His-Purkinje system and is often associated with structural heart disease. It also has been hypothesized that LBBB in itself can cause dyssynchronous heart failure. We used an electromechanical heart model with an integrated His-Purkinje system to simulate a healthy and a LBBB case. The LBBB affected only the His-Purkinje system and was not accompanied by other cardiovascular abnormalities. Hence, this case is called pure LBBB. For both simulations, we compared electrophysiological, hemodynamical and mechanical readouts. Our findings suggest that pure LBBB does not immediately lead to a severe change in cardiac output. As a consequence of mechanical dyssynchrony, we noticed a 2.5 % to 6.7 % absolute strain increase in the left ventricle. We hypothesize that this load imbalance causes remodeling over time, leading to a major reduction in ejection fraction. In line with clinical findings, our research indicates that electrical dyssynchrony immediately affects mechanics more than hemodynamics. These findings can provide insight and inform future research into the underlying mechanisms and efficacy of pacing treatments like cardiac resynchronization therapy.

Keywords: Dyssynchronous Heart Failure, Cardiac Resynchronization Therapy, Modeling, Hemodynamics

1 Introduction

Left bundle branch block (LBBB) is a conduction abnormality in the heart affecting the left bundle branch of the His-Purkinje system (HPS) with the direct consequence of delayed left ventricular activation. Although LBBB is mostly associated with structural heart disease and degenerative changes, it can also appear in absence of other cardiovascular abnormalities. LBBB can lead to heart failure and increases mortality in patients with underlying heart conditions [1]. One syn-

Carola Kruthoff, Jonathan Krauß, Tobias Gerach, Cristian Barrios Espinosa, Axel Loewe, Institute of Biomedical Engineering, Karlsruhe Institute of Technology (KIT), Fritz-Haber-Weg 1, 76131 Karlsruhe, Germany, e-mail: publications@ibt.kit.edu

Jorge Sánchez, Centro de Investigación e Innovación en Bioingenieria, Universitat Politècnica de València, Valencia, Spain

drome often associated with LBBB is dyssynchronous heart failure (HF_d). In HF_d , the dyssynchronous activation caused by LBBB leads to an uncoordinated contraction of the ventricles and a substantial decrease in pump function. A common treatment for HF_d patients is cardiac resynchronization therapy (CRT). The objective of CRT is to restore electrical synchrony via pacing and improve cardiac output. However, about one third of patients receiving CRT do not benefit long term [2]. Predicting the long term outcome of CRT remains difficult, since the relationship of acute and chronic effects of LBBB in HF_d is not well understood [2].

To gain a deeper understanding into these mechanisms, we simulated LBBB in an electromechanical whole heart model and assessed its immediate effect on cardiac mechanics and hemodynamics.

2 Methods

2.1 Electrophysiology

We simulated the electrical activation using the open cardiac electrophysiology simulator openCARP [3]. A whole heart mesh was generated from MRI data of a 33-year-old healthy volunteer [4]. The electrophysiology mesh had an average edge length of 0.8 mm. We generated the HPS (s. Figure 1) as a fractal tree, using anatomical structures and sites of earliest activation to guide the fractal growth [5]. The network was embedded in the subendocardial layer. The HPS was linked to the myocardium via Purkinje muscle junctions (PMJs): Each end of the network connected to 15 nodes in the myocardium via a resistive element. Apart from the PMJs, the network elements were isolated from the myocardium. We modeled the pure LBBB by setting the conductivities in the highlighted region in Figure 1 almost to zero (Table 1). Monodomain tissue conductivities for the ventricles and the HPS are listed in Table 1. We adopted the atrial conductivities from [6].

As output from monodomain simulations, we obtained transmembrane voltages (V_m) . The local activation time (LAT) of each node was defined as the time, when V_m crossed a threshold of -50 mV with a positive slope. In the atria, we applied a stimulus to a region of 413 nodes representing the sinoatrial node. In the ventricles, the HPS started at the atri-

Tab. 1: Conductivities (in S/m) in different ventricular regions and the His-Purkinje system. All conductivities are given as the half harmonic mean of the intra- and extracellular conductivity.

Region	normal	transversal	longitudinal
Subepicardium	0.098	0.182	0.28
Subendocardium	0.294	0.546	0.84
Purkinje system	12.15	12.15	12.15
LBBB	1e-32	1e-32	1e-32

oventricular node (AVN) (see Figure 1), which we stimulated 150 ms after the sinoatrial node activation.

To quantify the electrical dyssynchrony, we determined the total activation time (TAT) and the ventricular uncoupling (VEU) as proposed in [7]. The TAT denotes the time difference between earliest and latest site of activation. We calculated the TAT for both ventricles and each ventricle individually. The VEU marks the difference between the mean activation time of the right (RV) and left ventricle (LV). In both metrics, the septum was considered as part of the LV.

2.2 Mechanics and Hemodynamics

We modeled the mechanics and hemodynamics using the open source software CardioMechanics [8]. The mechanical simulation used a lower resolution version of the electrophysiology mesh (mean edge length: 3.17 mm) [4]. We applied different tension models and parameterizations:

- Configuration 1: Tension model by Niederer et al. [9];
 parametrization optimized for our heart geometry [10]
- Configuration 2: Tension model by Niederer et al. [9];
 default parametrization in CardioMechanics [8]

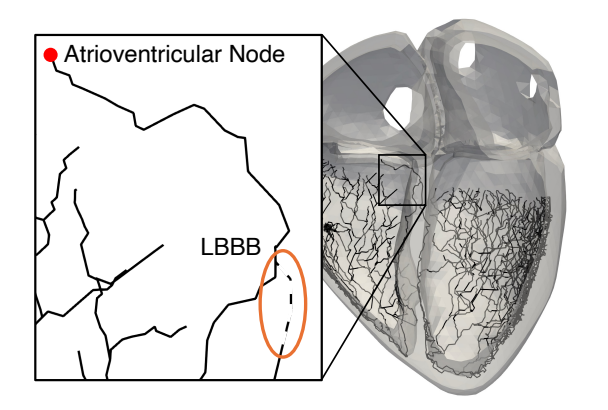


Fig. 1: His-Purkinje system and ventricle geometry. Inset: atrioventricular node as the point of stimulation marked in red and the LBBB as a dashed line.

- Configuration 3: Tension model by Land et al. [11] with calcium transient by Coppini; parametrization optimized for our heart geometry [6]
- Configuration 4: Tension model by Land et al. [11] with calcium transient by Coppini; default parametrization introduced by Land et al. [11]

To model hemodynamics, we used a 0D closed-looped model coupled to the mechanical system to guarantee volume consistency between the 3D and 0D models. The LATs of the electrophysiology simulation were mapped to the mesh of the mechanical geometry and used as an input for the tension model.

As a biomarker for mechanical changes, we computed the septal flash (SF), since it is used clinically as an indicator for mechanical dyssynchrony [12]. To measure SF, we imitated ultrasound M-mode tracking [12] by tracking points on the mid lateral region of the inner and outer surfaces of the LV free wall (LVfw) and the septum. The SF denotes the magnitude of the septum's leftward motion relative to the LV epicardium following its initial rightward motion, which occurs after the first onset of ventricular excitation (Figure 2).

We also evaluated the myofiber strain over time in the RV free wall (RVfw), LV free wall (LVfw) and the septum. To quantify the effects on hemodynamics, we computed the ejection fraction (EF) and the maximum rate of systolic pressure rise (dp/dt_{max}) for the LV.

3 Results

TAT and VEU indicate a major electrical dyssynchrony (Table 2). In LBBB, TAT_{RV} is prolonged by approx. 8 ms, while TAT_{LV} is almost doubled. This dyssynchrony is also reflected in the VEU for the LBBB case.

SF for all four configurations is shown in Table 3; myofiber strain for Configuration 1 is visualized in Figure 3. Higher SF for LBBB is apparent for all configurations. Me-

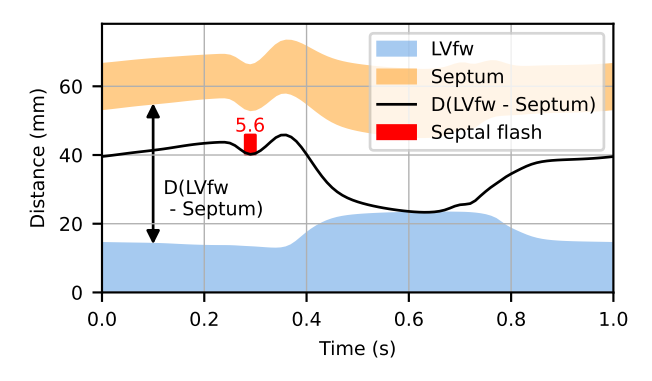


Fig. 2: Pseudo M-mode for the LBBB simulation with Configuration 1. The septal flash for this simulation is 5.6 mm.

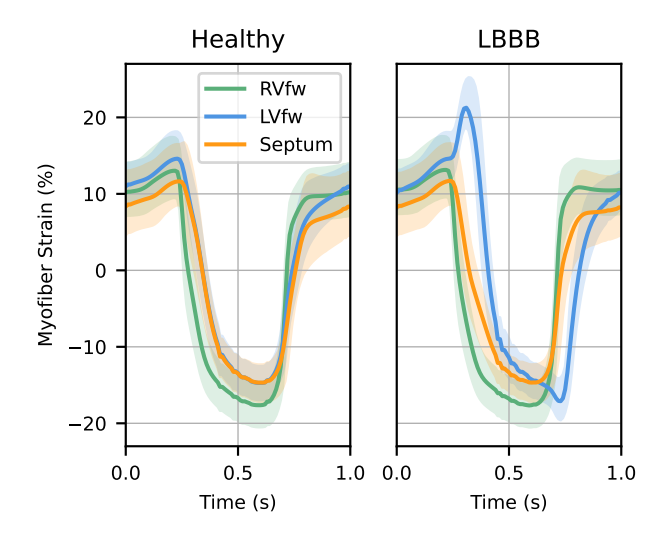


Fig. 3: Myofiber strain over time for Configuration 1 for the right ventricular free wall (RVfw), left ventricular free wall (LVfw) and the septum. Lines show the mean value, shaded areas represent interquartile range.

chanical dyssynchrony further manifests in the myofiber strain of the LVfw, which substantially increases in all configurations (2.9 % to 6.7 %) for LBBB before the LVfw contracts.

Hemodynamic metrics are displayed in Table 4. The change in EF is subtle for all configurations. dp/dt_{max} yielded relative changes of 15.8 % to 27.8 %, demonstrating the impact of electrical and mechanical dyssynchrony on hemodynamics.

4 Discussion

The electrical dyssynchrony in LBBB is due to the electrical impulse reaching the LV via the myocardium from the RV rather than through the HPS. The prolongation in TAT observed here is comparable to the wide QRS complex in patients

Tab. 2: Electrophysiological metrics (in ms). TAT - total activation time, VEU - ventricular uncoupling

Case	TAT _{RV + LV}	TAT _{RV}	TAT _{LV}	VEU	
Healthy	53.89	51.66	51.31	5.82	
LBBB	109.66	59.49	101.79	35.6	

Tab. 3: Septal flash (in mm) measured via pseudo M-mode.

Configuration	Healthy	LBBB
1	1.4	5.6
2	0.0	1.9
3	0.0	2.1
4	0.0	1.1

with LBBB [2]. We hypothesize that the substantial increase of strain in the LVfw happens because septum and RVfw contract earlier than the LVfw. The LVfw is stretched as a consequence. This strain increase marks an imbalance in mechanical load on the LV. Concerning the absolute values in hemodynamics, Configuration 2 and 4 yielded unphysiologically low EF. This can be expected, since the parameterizations are not optimized for our geometry. However, all simulations show a similar relative change in EF independent of parametrization.

The minimal change in EF for LBBB was unexpected. LBBB in HF_d patients is often accompanied by other pathologies [2], which in themselves can lead to reduced EF. However, there are studies focusing on patients with HF_d and LBBB in the absence of other cardiac diseases. In [13], patients with pure LBBB had a significantly lower EF (≈44 %) compared to healthy controls (\approx 63 %). In light of these unexpected findings, we compared our results to similar scenarios with other heart models. Meiburg et al. [14] modeled different CRT pacing strategies, where their best and worst performing strategy can be compared to our healthy and LBBB simulation, respectively. They measured a relative difference in EF of $\approx 1.5 \%$. Zingaro et al. [15] simulated a pure LBBB leading to a relative EF decrease of 1.28 %. Our and the reference simulations (here, [14], [15]) showed the immediate effect of pure LBBB, while the patients in [13] could be suffering from LBBB for a longer period of time. We hypothesize that the changes in mechanical load on the heart observed in our simulations lead to a structural remodeling over time. Hence, electrical and mechanical dyssynchrony are not directly responsible for the major reduction in EF. Accordingly, the pathologic decrease in pump function is caused by the remodeling.

To investigate this hypothesis, we explored clinical data on the acute effects of pure LBBB. Vernooy et al. [16] induced LBBB in healthy dogs via radiofrequency ablation. They showed an immediate decrease in cardiac output (-21.2 % after 30 min), but also stress that the effect of remodeling of the LV due to imbalanced strain results in a further reduction of EF. Schneider et al. [17] observed 55 patients before, during and after the onset of LBBB. In this group, 15 patients did not show any cardiovascular abnormalities before the onset of LBBB.

Tab. 4: Hemodynamic metrics for the left ventricle (LV). Relative values are normalized with respect to the corresponding healthy case.

Config.	LV Ejection Fraction (%)		LV dp/dt _{max} (mmHg/ms)			
	Healthy	LBBB	Δ (%)	Healthy	LBBB	Δ (%)
1	65.44	65.19	-0.4	1.65	1.39	-15.8
2	35.44	34.76	-1.9	1.15	0.83	-27.8
3	55	53.85	-2.1	2.28	1.87	-18.0
4	35.6	35.05	-1.5	1.47	1.18	-19.7

Out of these patients with pure LBBB, 60 % had no clinical abnormalities during the follow-up lasting several years. These findings indicate that, in humans, pure LBBB does not have to lead to an immediate or severe reduction in pump function. Vaillant et al. [18] and Sze et al. [19] both showed that patients with pure LBBB can have an EF close or equal to healthy individuals at the diagnosis of LBBB (50 to 55 %). In both studies, the EF decreased over time resulting in an indication for CRT.

If our in silico findings are confirmed in vivo, they have implications for pacing treatments like CRT. So far the acute electrophysiological and hemodynamic response during the implementation of CRT is used as a surrogate to predict long term effectiveness [20]. However, Prinzen et al. [20] concluded that restoration of pump function is not the defining factor for global recovery and mechanical response (e.g. strain data) should be considered instead. While their review examined CRT as a treatment of HF_d, we considered its root cause, coming to the same conclusion. Combining our in silico results with the work in [20], earlier application of CRT in patients with LBBB and only mildly reduced EF could be advised to prevent the remodeling. A limitation of our work is the focus on one LBBB scenario with a specific HPS representation on a single heart geometry.

5 Conclusion

We showed that pure LBBB without structural remodeling does not necessarily lead to an immediate, severe reduction in pump function in line with clinical human data. More data from patients during onset of LBBB are necessary to ultimately confirm our in silico findings.

Author Statement

This research was funded by Deutsche Forschungsgemeinschaft (DFG, German Research Foundation) – project #465189069 (LO 2093/6-2, SPP 2311). Jorge Sánchez is partially supported by the KIT Excellence Strategy via the Young Investigator Group Preparation Program. This work was performed on the computational resource bwUniCluster funded by the Ministry of Science, Research and the Arts and the universities of Baden-Württemberg, within the framework program bwHPC. Authors state no conflict of interest.

References

 Pérez-Riera A, et al. Left bundle branch block: Epidemiology, etiology, anatomic features, electrovectorcardiography,

- and classification proposal. Ann Noninvasive Electrocardiol 2018:24:e12572.
- [2] Dikdan S.J, et al. Dyssynchronous Heart Failure: A Clinical Review. Curr Cardiol Rep 2022;24:1957–1972.
- [3] Plank G, et al. The openCARP simulation environment for cardiac electrophysiology. Comput Methods Programs Biomed 2021;208:106223
- [4] Gerach T, et al. Four-Chamber Human Heart Model for the Simulation of Cardiac Electrophysiology and Cardiac Mechanics. https://doi.org/10.5281/zenodo.10526554
- [5] Correas M, et al. Automated Generation of Purkinje Networks in the Human Heart Considering the Anatomical Variability. Lec Notes in Comp Sci, Springer; 2023;13958:127–136.
- [6] Gerach T, et al. Differential effects of mechano-electric feedback mechanisms on whole-heart activation, repolarization, and tension. J Physiol 2024;602:4605-4624.
- [7] Ploux S, et al. Electrical dyssynchrony induced by biventricular pacing: Implications for patient selection and therapy improvement. Heart Rhythm 2015;12:782-791.
- [8] Gerach T, et al. CardioMechanics. Zenodo 2023. https://doi.org/10.5281/zenodo.8356660
- [9] Niederer S, et al. Length-dependent tension in the failing heart and the efficacy of cardiac resynchronization therapy. Cardiovasc Res 2011;89:336-343.
- [10] Gerach T, et al. The Impact of Standard Ablation Strategies for Atrial Fibrillation on Cardiovascular Performance in a Four-Chamber Heart Model. Cardiovasc Eng Technol 2023;14:296-314.
- [11] Land S, et al. A model of cardiac contraction based on novel measurements of tension development in human cardiomyocytes. J Mol Cell Cardiol 2017;106:68-83.
- [12] Walmsley J, et al. Septal flash and septal rebound stretch have different underlying mechanisms. Am J Physiol Heart Circ Physiol 2016;310:H394-H403.
- [13] Brunekreeft J, et al. Influence of left bundle branch block on left ventricular volumes, ejection fraction and regional wall motion. Neth Heart J 2007;15:89-94.
- [14] Meiburg R, et al. Comparison of novel ventricular pacing strategies using an electro-mechanical simulation platform. Europace 2023;25:euad144.
- [15] Zingaro A, et al. An electromechanics-driven fluid dynamics model for the simulation of the whole human heart. J Comp Phys 2024;504:112885.
- [16] Vernooy K, et al. Left bundle branch block induces ventricular remodelling and functional septal hypoperfusion. Eur Heart J 2005;26:91-98.
- [17] Schneider J, et al. Clinical-Electrocardiographic Correlates of Newly Acquired Left Bundle Branch Block: The Framingham Study. Am J Cardiol 1985;55:1332-1338.
- [18] Vaillant C, et al. Resolution of Left Bundle Branch Block-Induced Cardiomyopathy by Cardiac Resynchronization Therapy. JACC 2013;61:1089-1095.
- [19] Sze E, et al. Comparison of Incidence of Left Ventricular Systolic Dysfunction Among Patients With Left Bundle Branch Block Versus Those With Normal QRS Duration. Am J Cardiol 2017;120:1990-1997.
- [20] Prinzen F, et al. The "Missing" Link Between Acute Hemodynamic Effect and Clinical Response. J Cardiovasc Transl Res 2012;5:188-195.